Adsorption (2008) 14: 805–813
DOI 10.1007/s10450-008-9143-8

# Adsorbents for acetone in cyclohexane effuent employed in Ziegler-Natta catalyst process

**Maria A.C. Gollmann · Larissa B. Capeletti ·
Adriano G. Fisch · João Henrique Z. dos Santos ·
Márcia S.L. Miranda**

Received: 1 April 2007 / Revised: 31 July 2008 / Accepted: 12 September 2008 / Published online: 1 October 2008

**Abstract** Adsorption of acetone from cyclohexane on silica, alumina, coal, natural and leached chrysotile was investigated. Adsorption phenomenon was investigated by non-linear fitting, considering the Langmuir or Freundlich models. According to non-linear regression, coal present the highest $K_L$ (12.07) and $K_F$ (9.115) parameters. Silica and leached chrysotile exhibited similar behavior in terms of both $K_L$ and $K_F$ parameters. Alumina presented the highest adsorption capacity according to both Langmuir ($q_m = 58.689$) and Freundlich ($1/n = 0.844$) models. Non-supported Ziegler-Natta catalyst systems were shown to be more sensitive to acetone contamination. For the polymerization reactions carried on with contaminated solvent after the percolation through the adsorbents, good results were observed in the case of silica and alumina. Coal was not suitable for use in this catalyst system, probably due to leaching of organic components by the solvent (cyclohexane).

**Keywords** Adsorption · Acetone · Ziegler-Natta catalyst · Poison · Polymerization

## 1 Introduction

Adsorption has been found to be an efficient and economic process to remove contamination from industrial solvents. In recent years, minerals and their natural or modified forms have been investigated as adsorbent (Deosarkar and Pangarkar 2004; Li et al. 2005; Zulkali et al. 2006; Kumar and Silvanesan 2006). Examples, such as celestite (Ozkan et al. 2006), bentonite (Li et al. 2006), chrysotile (Valentin and Joekes 2006a), bauxite (Bhakat et al. 2006), talc mineral (Casanova et al. 2007), montmorillonite clays (Khaldoun et al. 2006) and kaolin (Wan and Liu 2006) have been recently reported in the literature.

The most commonly used property to design adsorption systems is the equilibrium information contained in adsorption isotherms, which are described by an equation, representing data collected after the adsorbate-containing fluid phase has been in contact with the adsorbent for sufficient time to reach equilibrium at a constant temperature. The different parameters and the underlying thermodynamic assumptions of theses equilibrium models often provide some insight about the sorption mechanism, and about the surface properties and the affinity of the adsorbent. The Langmuir and Freundlich models are the most commonly used isotherms to describe the adsorption equilibrium.

Currently sorption processes have been proved to be effective for removal of organic and inorganic pollutants from wastewater (Kumar and Sivanesan 2007). However, such processes can be extended for removal of impurities in the most varied systems. Some industrial processes demand specific control of contaminants. For instance, polymerization catalysts, such as Philips ($Cr/SiO_2$) or Ziegler-Natta ($TiCl_4/MgCl_2$) catalysts are strongly inhibited by alcohols, organic amines and sulfides (Eley et al. 1973; Ballard et al. 1976; Grayson and McDaniel 1991; Vizen et al. 1994). For Ziegler-Natta catalysts, traces of oxygenated compounds, in the ppb level, are enough to engender significant loss in catalytic activity.

---

M.A.C. Gollmann · L.B. Capeletti · A.G. Fisch ·
J.H.Z. dos Santos (✉)
Instituto de Química, UFRGS, Av. Bento Gonçalves, 9500
Porto Alegre, 91509-900, RS, Brazil
e-mail: jhzds@iq.ufrgs.br

M.S.L. Miranda
Braskem S.A., III Pólo Petroquímico, Via Oeste, Lote 05,
Triunfo, 95853-000, Brazil

In a previous paper, we developed an analytical method for determination of traces of acetone in cyclohexane effluents from petrochemical plants, based on solid phase microextraction (Gollmann et al. 2006). The present investigation aims at determining the acetone adsorption from cyclohexane on silica, alumina, coal, natural and leached chrysotile, correlating textural and chemical properties of the adsorbents with the adsorption capacity for acetone. The efficiency in retention of acetone by adsorbents was evaluated in employing percolated solvent, which was previously contaminated with traces of acetone, in ethylene polymerization by Ziegler-Natta catalysts.

## 2 Experimental

### 2.1 Materials

#### *2.1.1 Chemicals and reagents*

All employed chemicals were analytical reagent grade. For adsorption studies the solutions were prepared using acetone (Mallinckrodt, HPLC) and cyclohexane (VET). Coal (Indústria Carbonífera Rio Deserto Ltda, mined in Criciúma, Brazil), silica and alumina (purchased form Braskem, Camaçari, Brazil) were used as received. Chrysotile (kindly donated by SAMA, Mineração de Amianto Ltda, mined in Uruaçu, Brazil) was used in its natural form and also after acid treatment.

Polymerization experiments were performed under inert atmosphere (Argon) using the Schlenk technique. Titanium tetrachloride (Merck), acetone and diethylaluminium chloride toluene solution (DEAC) were used without purification. Cyclohexane and toluene were purified by distillation on metallic sodium and benzofenone. Silica Grace 948 ($255\ \mathrm{m}^2\ \mathrm{g}^{-1}$), employed for the preparation of Ziegler-Natta catalyst, was activated under vacuum ($P < 10^{-4}$ mbar) for 16 h at 110 °C. The support was cooled to room temperature under dynamic vacuum and stored under dried argon.

### 2.2 Methods

#### *2.2.1 Acid treatment*

Natural chrysotile (ca. 30 g) was mixed with hydrochloric acid solution (1000.0 mL–5.0 $\mathrm{mol\,L^{-1}}$). This suspension was kept under stirring for 24 hours at room temperatures yielding 15.0 g of product.

#### *2.2.2 Equilibrium adsorption studies*

A glass column ($L = 15$ cm; $\phi = 0.5$ cm) was packed with adsorbent (10 g). The column was loaded with adsorbate solution of a known concentration of contaminated solvent with acetone (range 1–200 ppm) in cyclohexane which was percolated through the column. The eluted solution was collected for further analysis by gas chromatography.

#### *2.2.3 Gas chromatographic analysis*

Analyses were carried out on a Hewlett-Packard HP5890, equipped with a flame ionization detector and a fused silica capillary column HP-1 (5 m × 0.53 mm × 2.65 µm) using He at 1 $\mathrm{mL\,min^{-1}}$ as carrier gas. Samples were injected in the splitless mode. The GC conditions were injector temperature: 290 °C; oven temperature program: initial temperature 50 °C for 2 minutes, then heating 10 $^\circ\mathrm{C\,min^{-1}}$ to 130 °C and finally isothermal at 130 °C for 2 min.

### 2.3 Adsorbents characterization

The adsorbents were characterized by a set of complementary techniques.

#### *2.3.1 Infrared spectroscopy (IR)*

Diffuse reflectance infrared Fourier transform spectroscopy (DRIFTS) was carried out using a FT-IR spectrometer equipped with a diffuse reflectance attachment (Bomen). Analyses at the transmittance modes were performed using KBr pressed technique, with 4 $\mathrm{cm^{-1}}$ of resolution, coadding 32 scans.

#### *2.3.2 Powder X-ray diffraction (XRD)*

The XRD data were collected on a Rigaku diffractometer with CuK$\alpha$ radiation (40 kV, 17.5 mA and 200 V). The phase development of chrysotile in the sample was examined in the scan range of 10–70°.

#### *2.3.3 $N_2$ adsorption-desorption analysis*

Nitrogen adsorption-desorption analyses were operated on a Micromeritics Gemini 2375 micropore analysis system. Samples (ca. 100 mg) were previously dehydrated under vacuum at 150 °C for 8 h. The analytical data were processed by the BET equation for the surface area and by the Barrett-Joyner-Halenda (BJH) method for pore size distribution.

#### *2.3.4 Scanning electron microscopy-energy dispersive X-ray analysis (SEM-EDX)*

Elemental analysis was carried on a Noran Instruments EDX system connected to a JEOL JSM 6300F scanning electron microscope, with an accelerating voltage of 10 kV. Samples were fixed on carbon tape on a stub and sputtered with gold before measurements.

**Table 1** Textural properties of the adsorbents

| | Silica | Coal | Alumina | Chrysotile | Leached chrysotile |
|---|---|---|---|---|---|
| *S* ($m^2/g$) | 646 | 406 | 213 | 23 | 294 |
| Dp (Å) | 22 | 27 | 59 | 54 | 39 |
| Vp ($cm^3/g$) | 0.20 | 0.26 | 0.31 | 0.02 | 0.29 |

### 2.4 Polymerization

#### *2.4.1 Preparation of supported catalyst*

Grafting experiments were performed under inert atmosphere using the Schlenk technique. Modified silica was prepared by impregnation, using activated silica (2.0 g) added to a toluene slurry containing $MgCl_2$ (50 wt% $MgCl_2/SiO_2$), at the temperature of 80 °C for 30 minutes under reflux. Solvent was removed under vacuum and a $TiCl_4$ cyclohexane solution (corresponding to 3.0% $Ti/SiO_2$) was added. The resulting slurry was stirred for 1 h at room temperature and filtered through a fritted disk. More details are reported elsewhere (Petry et al. 2006).

#### *2.4.2 Polymerization reactions*

Ethylene polymerization reactions were performed in 300 mL Pyrex glass reactor. The reactions were performed under Ar atmosphere using cyclohexane as solvent (150 $dm^3$), 1.6 atm of ethylene for 30 minutes at 60 °C. DEAC was employed as the cocatalyst (Al/Ti = 200). For the non-supported $TiCl_4$ catalyst system the following conditions were employed: $[M] = 10^{-3}$ mol/L and Al/Ti = 5, while for supported ones: $[M] = 10^{-5}$ mol/L and Al/Ti = 200. The solvent was contaminated with acetone (0–80 ppm). In reactions using adsorbents, the contaminated solvent (50 ppm) was percolated through the adsorbent (2.0 g) column under inert atmosphere and transferred into the reactor.

## 3 Results and discussion

The employed phases were characterized by a series of volumetric and spectroscopic techniques in order to get some information about their textural, morphological and chemical properties.

### 3.1 Adsorbents' characterization

Table 1 shows the textural properties determined by nitrogen adsorption, calculated by the BET and the BJH methods (Webb and Orr 1997).

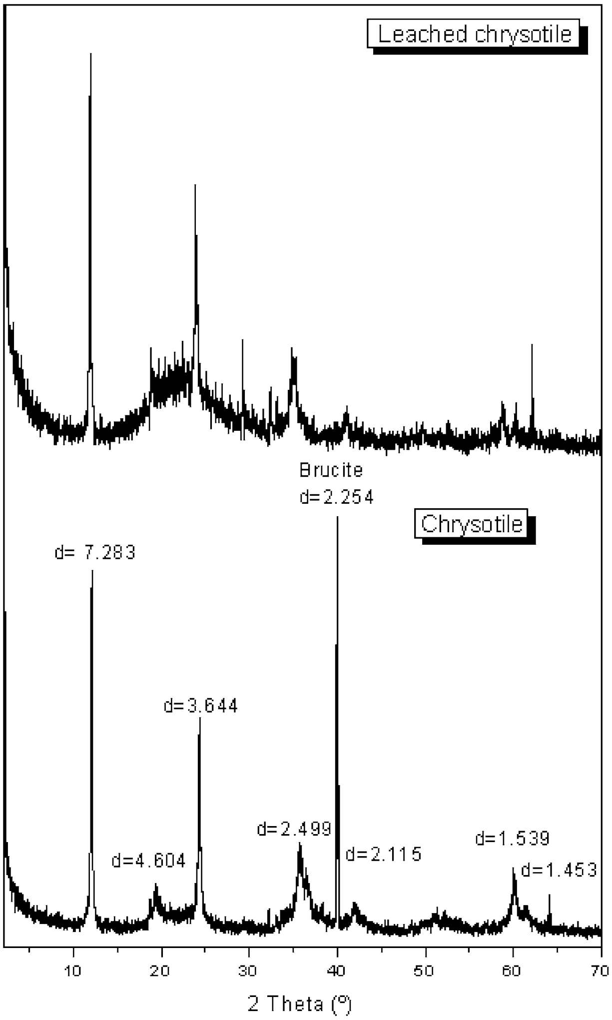

**Fig. 1** XRD patterns of natural and leached chrysotile

According to Table 1, silica is the adsorbent with the highest specific area, followed by coal and alumina. Chrysotile presents a low specific area, but after the acid treatment there is significant increase in it, being comparable to that observed in the case of alumina. Pore diameter was in the range of 20–60 Å, being higher in the case of alumina and of natural chrysotile. In the case of leached chrysotile, volume of the micropore increased after acid treatment, being comparable to that of alumina and coal. It is worth noting that acid treatment aims to remove brucite ($Mg(OH)_2$) from the external surface, remaining silica (Mendelovici and Frost 2005; Wypych et al. 2005; Valentin and Joekes 2006b; Bernstein and Hoskins 2006). Samples of natural and leached chrysotile were characterized by XRD (Fig. 1).

According to Fig. 1, all the peaks can be assigned to natural chrysotile ($3MgOSiO_2 \cdot 2H_2O$), excepting that at $2\theta = 40°$ which was attributed to brucite ($Mg(OH)_2$) (Bernstein and Hoskins 2006). After acid treatment, there is a signal loss at that phase assigned to brucite. Normally acid

**Fig. 2** DRIFTS spectra of: (**a**) natural and (**b**) leached chrysotile

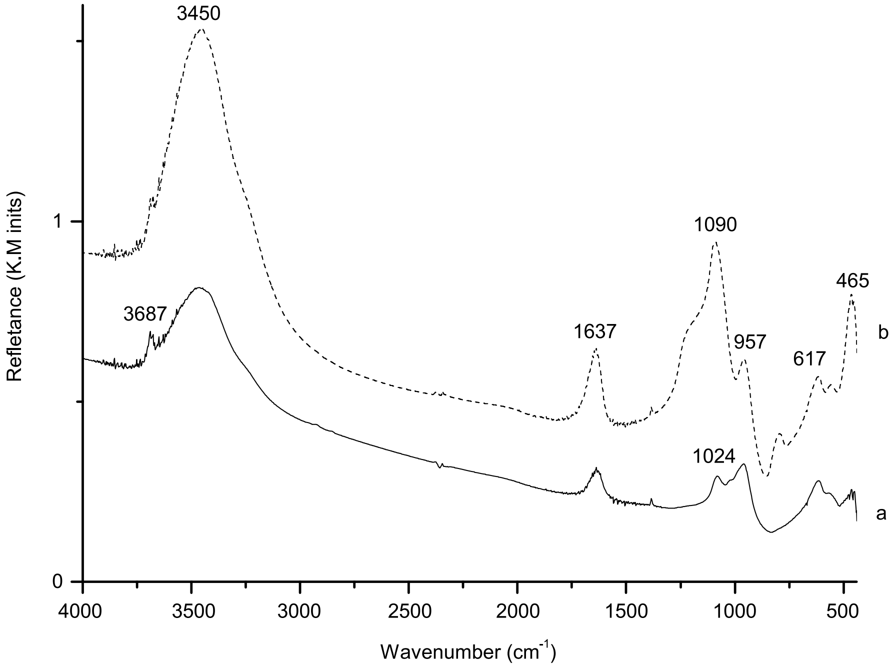

treatment results in nano-fibriform silica, completely amorphous (Mendelovici and Frost 2005; Wypych et al. 2005; Valentin and Joekes 2006b). In the present case, the XRD pattern confirms that the crystalline structure of chrysotile is maintained, associate to an amorphous structure, centered at $2\theta = 20°$, attributed to amorphous silica (Xu et al. 2006; Samadi-Maybodi and Atashabozorg 2006; Cheng et al. 2006).

Chemical groups on natural and leached chrysotile were identified by DRIFTS, as shown in Fig. 2. The characteristic band at 3687 cm$^{-1}$(spectrum **a** of Fig. 2) is attributed to $\nu$(O–H) stretching bond attached to magnesium center. After acid treatment, this band is significantly reduced, probably due to brucite phase removal (spectrum **b** of Fig. 2), indicating that brucite sheet of chrysotile might be partially destroyed.

In Fig. 2, the broad band between 2750 and 3600 cm$^{-1}$ can be attributed to adsorbed water. The peak at 1090 cm$^{-1}$ is attributed to the vibration modes of Si–O network that consists of Si–O–Si and O–Si–O, and the Si–O stretching peak which is vertical to the prolongation of the fiber, was undetected at 1024 cm$^{-1}$ due to natural chrysotile tetrahedral sheets attacked by HCl. The peak at 617 cm$^{-1}$ was identified as the terminal Si–OH deformation band, the Si–O–Si bending peak was detected at 465 cm$^{-1}$ (Wypych et al. 2005; Wang et al. 2006; Halma et al. 2006; Falini et al. 2006).

Chemical composition of chrysotile and leached chrysotile were further analyzed by SEM-EDX. The results are show in Table 2.

**Table 2** Elemental analysis of chrysotile and leached chrysotile

| | Element (%) | | | |
|---|---|---|---|---|
| | O | Mg | Si | Fe |
| Chrysotile | 59.85 | 18.85 | 18.23 | 2.95 |
| Leached chrysotile | 66.55 | 0.35 | 33.10 | – |

From the SEM-EDX data, there is magnesium loss after the acid treatment; Mg was practically completely removed. Fe is present in natural chrysotile, probably as a contaminant, but it was removed after acid treatment.

The morphologies of commercial adsorbents, namely silica, alumina and coal, were characterized by SEM. Figure 3 shows the micrographs.

Among the investigated adsorbents, silica is the adsorbent which surface is the most homogeneous. Alumina surface is characterized by a more spongy texture, while coal shows a very heterogeneous surface. Figure 4 shows the micrograph of leached chrysotile.

According to Fig. 4, some tubular structure can be observed, indicating that the fibrous morphology was kept after leaching. Similar images have been reported in the literature (Wypych et al. 2005; Halma et al. 2006; Falini et al. 2006; Xu et al. 2006).

### 3.2 Adsorptions isotherms

The adsorption process was quantitatively evaluated for all adsorbents by determining the adsorption isotherms, where $q_e$ is the amount of adsorbed acetone per unit of mass of ad-

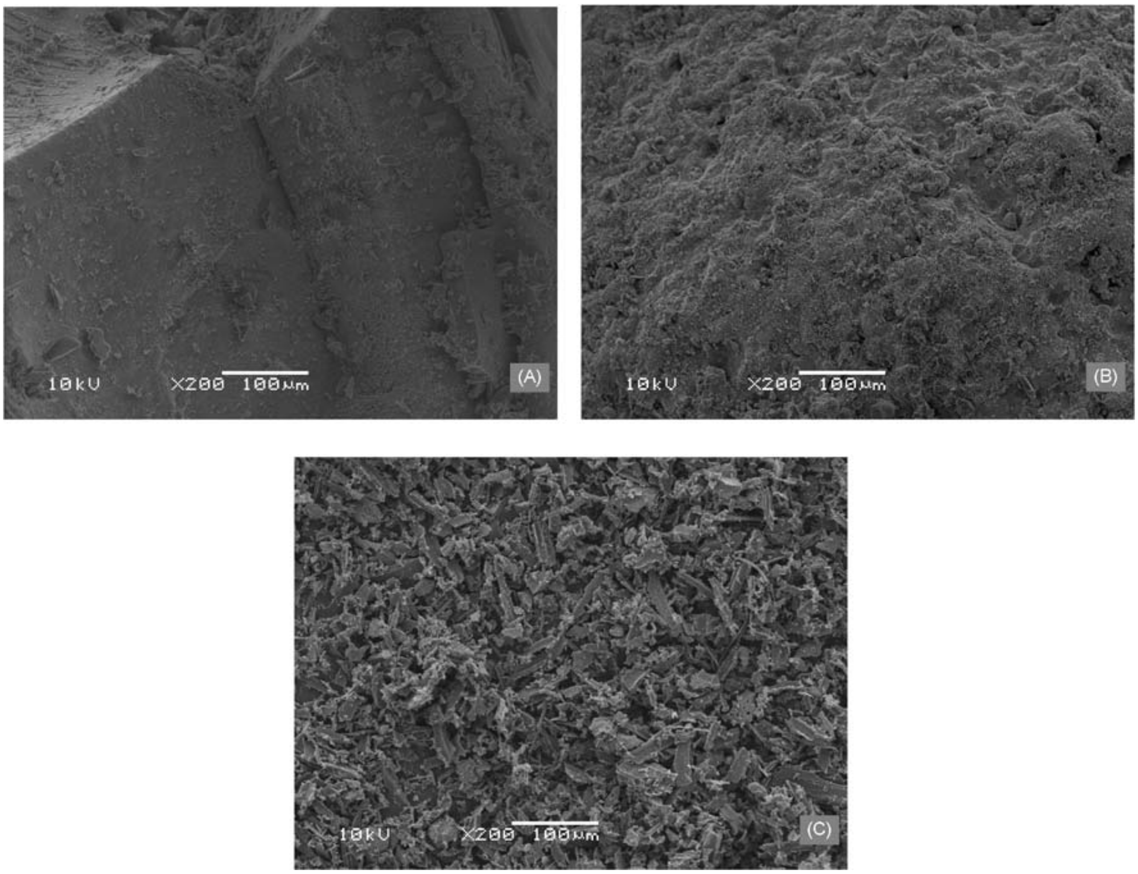

**Fig. 3** Micrographs of commercial adsorbents employed in adsorptions process. Magnitude: 200×: (**A**) silica, (**B**) alumina and (**C**) coal

sorbent (silica, alumina, coal, chrysotile and leached chrysotile) in (mg/g) and $C_e$ is the equilibrium concentration of acetone in cyclohexane ($\text{mg}\,\text{L}^{-1}$).

The adsorption isotherms were interpreted according to the adsorption models of Freundlich (1) and Langmuir (2):

$$q_e = k_F C_e^{\frac{1}{n}}, \tag{1}$$

$$q_e = \frac{q_m k_L C_e}{1 + k_L C_e}. \tag{2}$$

Fitting via nonlinear regression was than evaluated. Therefore, the parameters of the nonlinear model were estimated via *lsqnonlin* function from MATLAB®, which solves the optimization problem by means of Levenberg-Marquardt algorithm with line-search according to (3), where *fo* is the objective function to minimize and $x$ the manipulated variable vector.

$$\min_x \quad fo$$
$$fo = \sum_i (q_{e\_\exp,i} - q_{e\_pred,i}(x))^2. \tag{3}$$

The resulting isotherms, considering the non-linear fitting, are shown in Fig. 5.

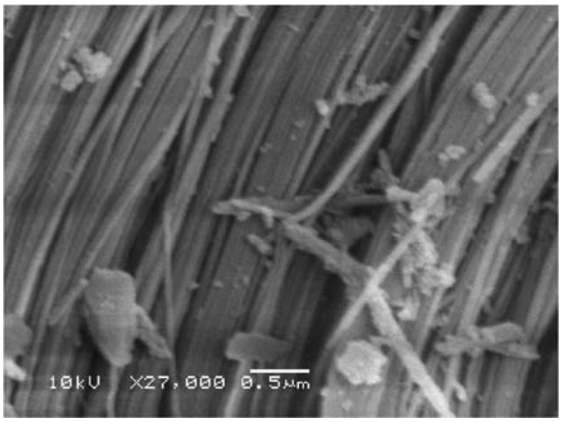

**Fig. 4** Leached chrysotile micrograph. Magnitude: 2200×

Based on the Freundlich model (Fig. 5a), leached chrysotile (silica-based material), coal and silica were shown to exhibit good capacity for acetone from cyclohexane adsorption. Alumina was not shown to be a good adsorbent. Nevertheless, according to the Langmuir model (Fig. 5b), is the best adsorbent in comparison to the other ones. Natural chrysotile was shown to be less efficient, independent of the model.

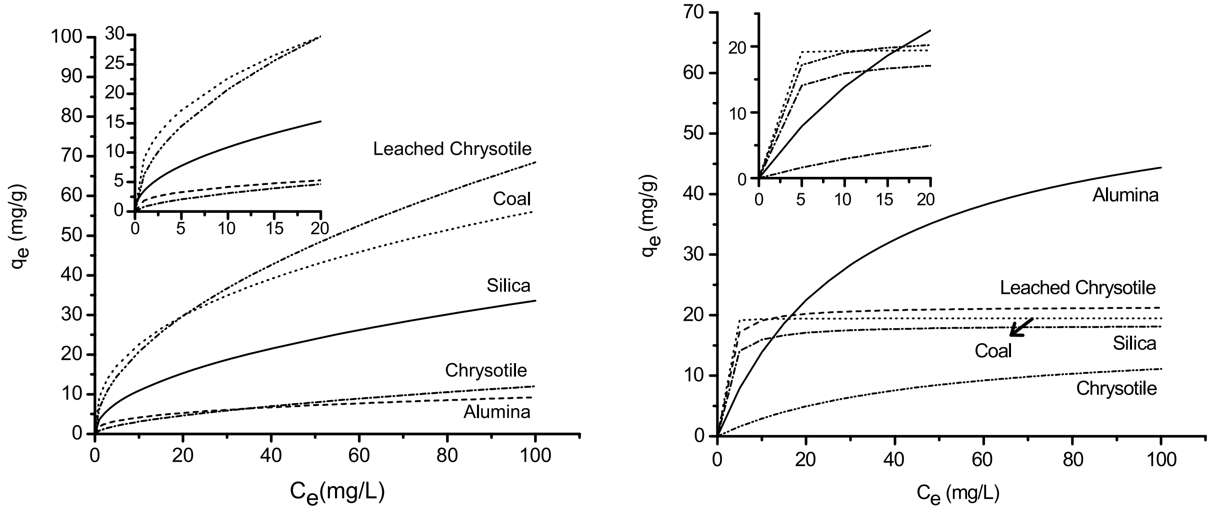

(a) (b)

**Fig. 5** Adsorption isotherms for acetone in cyclohexane on the investigated adsorbents determined by non-linear fitting using (**a**) Langmuir and (**b**) Freudlich models. Low concentration region in the inset

**Table 3** Isotherm parameters obtained by using non-linear regression

| Sorbent | Langmuir<br>$q_e = \frac{q_m k_L C_e}{1+k_L C_e}$ | Freundlich<br>$q_e = k_F C_e^{\frac{1}{n}}$ |
|---|---|---|
| Silica | $q_m = 18.391 \pm 0.78$ | $k_F = 3.551 \pm 0.75$ |
| | $k_L = 0.649 \pm 0.79$ | $1/n = 0.488 \pm 0.76$ |
| | $r^2 = 0.999$ | $r^2 = 0.998$ |
| Alumina | $q_m = 58.689 \pm 0.16$ | $k_F = 1.889 \pm 3.44$ |
| | $k_L = 0.031 \pm 0.16$ | $1/n = 0.844 \pm 13.73$ |
| | $r^2 = 0.996$ | $r^2 = 0.996$ |
| Coal | $q_m = 19.488 \pm 193.89$ | $k_F = 9.115 \pm 8.74$ |
| | $k_L = 12.072 \pm 193.99$ | $1/n = 0.3948 \pm 1.29$ |
| | $r^2 = 0.994$ | $r^2 = 0.994$ |
| Chrysotile | $q_m = 16.180 \pm 0.02$ | $k_F = 0.794 \pm 0.04$ |
| | $k_L = 0.022 \pm 0.02$ | $1/n = 0.590 \pm 0.35$ |
| | $r^2 = 0.993$ | $r^2 = 0.997$ |
| Leached chrysotile | $q_m = 21.465 \pm 13.19$ | $k_F = 6.303 \pm 2.67$ |
| | $k_L = 0.807 \pm 13.20$ | $1/n = 0.518 \pm 0.93$ |
| | $r^2 = 0.992$ | $r^2 = 0.989$ |

The isotherm parameters of silica, alumina, coal, chrysotile and leached chrysotile considering non-linear regression are presented in Table 3.

According to Table 3, taking into account the correlation factor ($r^2$), both Langmuir and Freundlich models accounts for the adsorption isotherms. Considering Langmuir parameters, the highest values of equilibrium constant ($K_L$) was observed for coal. This constant describes the energy of adsorption and affinity of acetone for this adsorbent. Much lower and comparable values were observed in the case of silica and leached chrysotile (which can be considered as a nanosilica fiber), and even lower for the two other sorbents. The $q_m$ parameter measures the monolayer (maximum) adsorption capacity. According to Table 3, $q_m$ value is much higher for alumina.

Concerning Freundlich isotherm parameters, the highest $K_F$ value, which indicates the distribution of active sites, was observed for coal. Silica and leached chrysotile presented lower and compared valuables. The adsorption capacity ($1/n$), as in the case of Langmuir model, was higher for alumina.

### 3.3 Polymerizations

The robustness of supported and non-supported Ziegler-Natta catalytic system was evaluated by ethylene polymerization reactions, using solvent contaminated with acetone (Fig. 6).

For both systems, catalyst activity was shown to be reduced as traces of acetone are added to the system. Comparing both catalyst systems, the non-supported ones were more sensitive to poisoning, since a steep reduction in catalyst activity is observed even for very low acetone contents. On the other hand, the reduction in catalyst activity is less abrupt in the case of supported catalysts.

The differences observed for both catalyst sites might be due to the availability of coordinating sites on each catalyst system as proposed in Scheme 1.

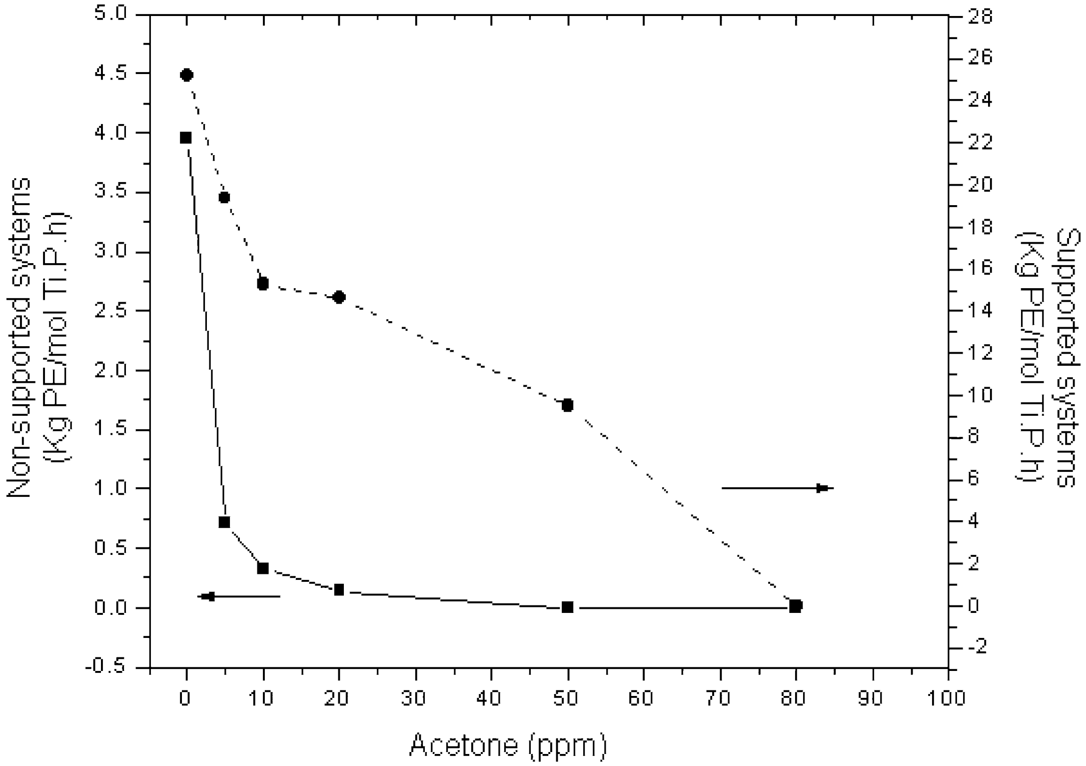

**Fig. 6** Catalytic activity (■) non-supported and (●) supported Ziegler-Natta catalyst systems in ethylene polymerization

**Scheme 1**

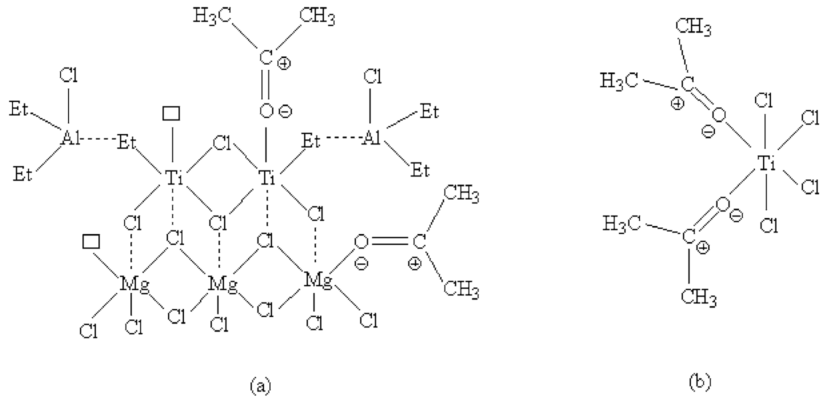
(a) (b)

Scheme 1 represents the available sites of non-supported and supported Ziegler-Natta catalyst systems. For the non-supported $TiCl_4$ systems, the only available site is on Ti center. On this site, there is a competition between ethylene and acetone for coordination (the irreversible coordination onto Ti obstruct olefin coordination; therefore, reducing the catalytic activity). When $TiCl_4$ is supported onto $MgCl_2$ surface, the Mg ions of the support can present vacant sites acting as Lewis acid sites, on which acetone molecules can also coordinate (Soga and Shiono 1997). In the case of the supported systems, acetone has not only Ti as possibility for coordination, but also the Mg surface on the support. This might explain the differences in catalyst activity observed for both type of systems.

The non-supported Ziegler-Natta catalytic system was evaluated with cyclohexane containing traces of acetone after percolation through the investigated adsorbents. Figure 7 shows the results expressed in terms of percentage of total catalyst activity (%) without contamination (**A**) and with 50 ppm of acetone contaminate (**B**).

As shown in Fig. 7, there is a 60% loss of catalytic activity, after the addition of 50 ppm of acetone. For the polymerization reactions carried on with contaminated solvent after the percolation through the adsorbents, good results were observed in the case of silica and alumina. A reduc-

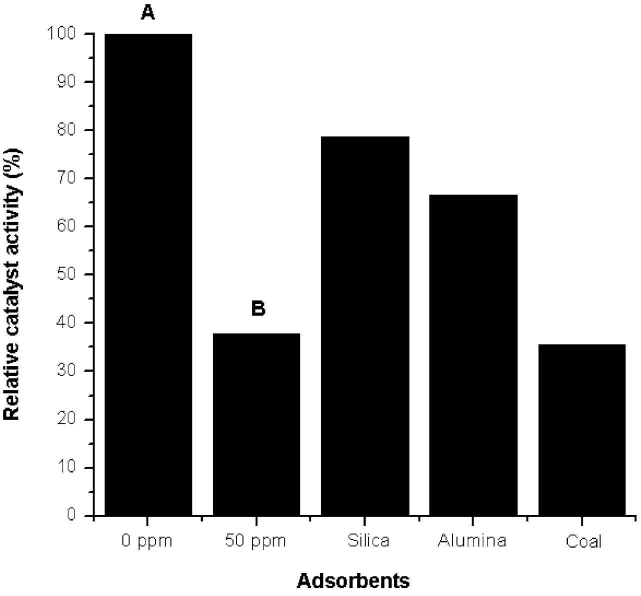

**Fig. 7** Activity of $TiCl_4/MgCl_2$ catalyst in ethylene polymerization supported systems, using solvent containing acetone (50 ppm), after percolation through the adsorbent

tion of only 20% was observed in the case of silica, showing the potential capability of these adsorbents for such contaminated systems. Surprisingly, coal, in spite of offering good adsorption properties, was not suitable for use in this catalyst system. The resulting polymer was black. Furthermore, catalyst activity was much reduced, probably due to organic groups such as carboxyl, quinone, hydroxyl, carbonyl, lactone, carboxylic anidride released by coal (Yang 2003).

## 4 Conclusion

The determination of acetone adsorption isotherms form cyclohexane on inorganic phases allowed us to identify, preliminarily, that silica, alumina, coal and leached chrysotile presented as potential adsorbents. Natural chrysotile showed lesser values of adsorption capacity. The nonlinear regression analysis using Langmuir or Freundlich isotherm suggests that coal presents the best adsorption capacity, followed by alumina. Silica and leached chrysotile have shown similar adsorption properties.

Catalytic activity of Ziegler-Natta systems using cyclohexane contaminated with acetone showed that non-supported systems were more prone to poisoning. In supported systems, the reduction in catalyst activity was less abrupt. A possibility is that when $TiCl_4$ is supported onto the $MgCl_2$ surface, the acetone molecules can dispose of the vacant sites presents on the support to coordinate, engendering lower catalytic activity.

For the polymerization reactions carried on with the contaminated solvent after the percolation through the adsorbents, good results were observed in the case of silica and alumina. A reduction of 20 to 30% was observed in catalytic activity losses, respectively.

**Acknowledgements** The authors acknowledge the financial support by Braskem and Instituto UNIEMP. Mr. William Bretas Linares from SAMA is specially thanked for providing chrysotile samples. CNPq and FAPERGS/PRONEX are also thanked for partial support.

## References

Ballard, D.G.H., Burnham, D.R., Twose, D.L.: The measurement of the equilibrium constant for the formation of a complex between olefins and group IVA metal alkyls. J. Catal. **44**, 116–125 (1976)

Bernstein, D.M., Hoskins, J.A.: The health effects of chrysotile: Current perspective based upon recent data. Regul. Toxicol. Pharmacol. **45**, 252–264 (2006)

Bhakat, P.B., Gupta, A.K., Ayoob, S., Kundu, S.: Investigations on arsenic(V) removal by modified calcined bauxite. Colloids Surf. A **281**, 237–245 (2006)

Casanova, H., Orrego, J.A., Zapata, J.: Oil absorption of talc minerals and dispersant demand of talc mineral non-aqueos dispersion as a function of talc content: a surface chemistry approach. Colloids Surf. A **299**, 38–44 (2007)

Cheng, Q., Plavlinek, V., Li, C., Lengalova, A., He, Y., Saha, P.: Synthesis and characterization of new mesoporous material with conducting polypyrrole confined in mesoporous silica. Mater. Chem. Phys. **98**, 504–508 (2006)

Deosarkar, S.P., Pangarkar, V.G.: Adsorptive separation and recovery of organics from PHBA and SA plant effluents. Sep. Purif. Technol. **38**, 241–254 (2004)

Eley, D.D., Rochester, C.H., Scurrell, M.S.: The polymerisation of ethylene on chromium oxide catalysts: III. An infrared study of the adsorption of carbon monoxide on active catalyst. J. Catal. **29**, 20–30 (1973)

Falini, G., Foresti, E., Lesci, I., Lunellu, B., Sabatino, P., Roveri, N.: Interaction of bovine serum albumin with chrysotile: Spectroscopic and morphological studies. Chem. Eur. J. **12**, 1968–1974 (2006)

Gollmann, M.A.C., Peralba, M.C.R., Pizzolato, T.M., dos Santos, J.H.Z., Cavalcanti, M.J.R.: Use of solid phase microextraction for the detection of acetone in cyclohexane effluent. Colloids Surf. A **286**, 134–137 (2006)

Grayson, M.E., McDaniel, M.P.: Sulfide poisoning of ethylene polymerization over Phillips Cr/silica catalyst. J. Mol. Catal. A: Chem. **65**, 139–144 (1991)

Halma, M., Bail, A., Wypych, F., Nakagaki, S.: Catalytic activity of anionic iron(III) porphyrins immobilized on grafted disordered silica obtained from acidic leached chrysotile. J. Mol. Catal. A: Chem. **243**, 44–51 (2006)

Khaldoun, A., Wegdam, G.H., Eiser, E., Kerkeb, M.L., Duran, J.D.G., González-Caballero, F., Bonn, D.: Influence of heavy metals adsorption on the surface-energy properties of fluorinated montmorillonite clays "Rassoul". Colloids Surf. A **290**, 1–6 (2006)

Kumar, K.V., Silvanesan, S.: Equilibrium data, isotherm parameters and process design for partial and complete isotherm of methylene blue onto activated carbon. J. Hazard. Mater. **134**, 237–244 (2006)

Kumar, K.V., Sivanesan, S.: Sorption isotherm for safranin onto rice husk: Comparison of linear and non-linear methods. Dyes Pigments **72**, 130–133 (2007)

Li, T., Wang, C., Liu, X., Zheng, J., Wang, H.: Characteristics of mesocarbon microbeads generated from a coal tar pitch with addition of micro-alumina powder. Fuel Process. Technol. **87**, 77–83 (2005)

Li, J., Zhu, L., Cai, W.: Characteristics of organobentonite prepared by microwave as a sorbent to organic contaminants in water. Colloids Surf. A **281**, 177–183 (2006)

Mendelovici, E., Frost, R.L.: Pioneer studies on HCl and silylation treatments of chrysotile. J. Colloid Interface Sci. **289**, 597–599 (2005)

Ozkan, A., Ucbeyiaty, H., Aydogan, S.: Shear flocculation of celestite with anionic surfactants and effects of some inorganic dispersants. Colloids Surf. A **281**, 92–98 (2006)

Petry, C.F., Capeletti, L.B., Stedile, F.C., dos Santos, J.H.Z., Pozebon, D.: Determination of titanium and vanadium in Ziegler-Natta catalysts by inductively coupled plasma atomic emission spectrometry. Anal. Sci. **22**, 855–859 (2006)

Samadi-Maybodi, A., Atashabozorg, E.: Quantitative and qualitative studies of silica in different rice samples grown in north of Iran using UV–vis, XRD and IR spectroscopy techniques. Talanta **70**, 756–760 (2006)

Soga, K., Shiono, T.: Ziegler-Natta catalysts for olefin polymerizations. Prog. Polym. Sci. **22**, 1503–1546 (1997)

Valentin, I.B., Joekes, I.: Adsorption of sodium dodecylsulfate on chrysotile. Colloids Surf. A **290**, 106–111 (2006a)

Valentin, I.B., Joekes, I.: Adsorption of sodium dodecylsulfate on chrysotile. Colloids Surf. A: Physichochem. Eng. **290**, 106–111 (2006b)

Vizen, E.I., Rishina, L.A., Sosnovskaja, L.N., Dyachkowsky, F.S., Dubnikova, I.L., Ladygina, T.A.: Study of hydrogen effect in propylene polymerization on (with) the $MgCl_2$-supported Ziegler-Natta catalyst—part 2. Effect of $CS_2$ on polymerization centres. Eur. Polym. J. **30**, 1315–1318 (1994)

Wan, Y., Liu, C.: The effect of humic acid on the adsorption of REEs on kaolin. Colloids Surf. A **290**, 112–127 (2006)

Wang, L., Lu, A., Wang, C., Zheng, X., Zhao, D., Liu, R.: Nanofibriform production of silica from natural chrysotile. J. Colloid Interface Sci. **295**, 436–439 (2006)

Webb, P.A., Orr, C.: Analytical Methods in Fine Particle Technology. Micromeritcs, Norcross (1997)

Wypych, F., Adad, L.B., Mattoso, N., Marangon, A.A.S., Schreiner, W.H.: Synthesis and characterization of disordered layered silica obtained by selective leaching of octahedral sheets from chrysotile and phlogopite structures. J. Colloid Interface Sci. **283**, 107–112 (2005)

Xu, Q., Fan, H., Guo, Y., Cao, Y.: Preparation of titania/silica mesoporous composites with activated carbon template in supercritical carbon dioxide. Mater. Sci. Eng. A **435–436**, 158–162 (2006)

Xu, J., Li, X., Zhou, W., Ding, L., Jin, Z., Li, Y.: J. Porous Mater. **13**, 275–279 (2006)

Yang, R.T.: Adsorbents. Fundamentals and Applications. Wiley, New York (2003)

Zulkali, M.M.D., Ahamad, A.L., Norulakmal, N.H.: Oryza sativa L. husk as heavy metal adsorbent: Optimization with lead as model solution. Bioresour. Technol. **97**, 21–25 (2006)